VOC absorption in supramolecular deep eutectic solvents: Experiment and molecular dynamic studies

Chengmin Gui, Pedro Villarim, Zhigang Lei, Sophie Fourmentin

Chemical Engineering Journal 481 (2024) 148708

Contents lists available at ScienceDirect

Chemical Engineering Journal

journal homepage: www.elsevier.com/locate/cej

VOC absorption in supramolecular deep eutectic solvents: Experiment and molecular dynamic studies

Chengmin Gui [a,b], Pedro Villarim [b], Zhigang Lei [a,c], Sophie Fourmentin [b,*]

[a] State Key Laboratory of Chemical Resource Engineering, Beijing University of Chemical Technology, Box 266, Beijing 100029, China
[b] Univ. Littoral Côte d'Opale, UR 4492, UCEIV, Unité de Chimie Environnementale et Interactions sur le Vivant, F-59140 Dunkerque, France
[c] School of Chemistry and Chemical Engineering/State Key Laboratory Incubation Base for Green Processing of Chemical Engineering, Shihezi University, Shihezi 832003, China

ARTICLE INFO

Keywords:
Deep eutectic solvents
Supramolecular
Volatile organic compounds
Cyclodextrins
Absorption mechanism
Molecular dynamic

ABSTRACT

The absorption of volatile organic compounds (VOCs) using supramolecular deep eutectic solvents (SUPRADES), composed of randomly methylated β-cyclodextrin (RAMEB) and conventional organic solvents, was systematically investigated from vapor-liquid experiments to molecular dynamic simulations. The obtained partition coefficients suggest that the combination of RAMEB and ethylene glycol (REG, mole ratio 1:40) significantly improves the absorption ability of ethylene glycol (EG), making REG even the most efficient absorbent for chloroform and limonene. By studying the key factors affecting the absorption process, we found that increasing the concentration of VOCs in the gas phase, lowering the absorption temperature or reducing the water content of the absorbent are effective in improving absorption. Regeneration test shows that the absorption ratio of chloroform using REG is maintained around 99% under six absorption–desorption cycles, highlighting its high absorption efficiency and stability. The absorption mechanism was then deeply explored by molecular dynamic simulation. It was found that the hydrogen bond between RAMEB and EG hinders the aggregation of neighboring RAMEB molecules, helping RAMEB to form stable and homogeneous solvent with EG. In addition, the interaction energy analysis demonstrates that van der Waals forces contribute the most to the absorption of chloroform by REG. Finally, the radical distribution function analysis was used to visualize the 2-dimensional molecule distribution of SUPRADES systems and the spatial distribution analysis verified the formation of RAMEB/chloroform inclusion complexes in the absorption process. The obtained results indicate that REG is a highly efficient and easy recyclable solvent for VOCs absorption.

1. Introduction

Global challenges in atmosphere and water protection have created a great demand for highly efficient capture of volatile organic compounds (VOCs) from industrial waste gas, as some VOCs are not only among the most common air and water pollutants, but also potential human teratogens and carcinogens [1,2]. Various techniques, such as absorption [3], adsorption [4], condensation [5] and catalytic combustion [6], were proposed to destroy or recover VOCs with some advantages and limitations. Solvent absorption is a promising VOCs recovery technique because of its simple operation process and large treatment capacity [7]. It should be noted that using traditional organic solvents as absorbents has several drawbacks, such as corrosion, thermal decomposition losses and energy-intensive solvent recovery [8]. Adsorption is characterized by high VOC removal ratio and good thermal stability [9]. However, the deactivated adsorbents may cause secondary pollution, and frequent switching of adsorption and desorption operations affects the adsorption efficiency [10]. The condensation method is almost not affected by the surrounding temperature and has low equipment investment [11]. However, it is difficult to treat exhaust gas containing low concentrations of VOCs, and the concentration of VOCs after treatment is high [12]. Therefore, it is generally used as a pretreatment method. Catalytic combustion can completely eliminate VOCs and has low operating costs [13]. Unfortunately, the high-temperature operating conditions place strict requirement on the equipment, and the treatment of chlorinated VOCs easily produces hydrogen chloride and high-molecular-weight chlorinated by-products [14].

In the current era, VOCs absorption technology has received

* Corresponding author.
E-mail address: lamotte@univ-littoral.fr (S. Fourmentin).

https://doi.org/10.1016/j.cej.2024.148708
Received 20 November 2023; Received in revised form 3 January 2024; Accepted 9 January 2024
Available online 12 January 2024

extensive attention due to the rapid development of green solvents, such as ionic liquids (ILs) [15,16], and deep eutectic solvents (DESs) [17,18]. The unique thermochemical properties of ILs, such as negligible volatility, good thermal stability and designable structure, make them attractive VOC absorbents [19]. DESs retain the common advantages of ILs, and have lower toxicity and easier preparation process, facilitating their industrial application in the VOCs treatment [20]. In the selection of hydrogen bond acceptors (HBA) for VOCs absorption, the majority of studies have focused on choline chloride, quaternary ammonium salts and quaternary phosphonium salts [21,22]. The hydrogen bond donors (HBDs) paired with HBAs are mainly glycols, carboxylic acids and amides [23–25]. To the best of our knowledge, there are far fewer studies on the use of supramolecular DESs to absorb VOCs than on the use of conventional DESs [26].

As a type of extensively studied supramolecule, cyclodextrins (CDs) are composed of a series of cyclic oligosaccharides produced by the enzymatic degradation of starch [27]. CDs can encapsulate guests through their hydrophobic inner cavities, thereby improving the solubility, permeability and stability of the included molecules [28]. The most common CDs are the native α-CD, β-CD and γ-CD, which consist of six, seven and eight glucosyl units, respectively, linked by 1,4-α-glycosidic bonds [29,30]. Among the β-CD derivatives, randomly methylated β-cyclodextrin (RAMEB) shows great potential for VOCs capture [31,32]. More importantly, their methylated hydrophilic outer surface improves the miscibility with water and other organic solvents, making them easier to prepare as liquid DESs at room temperature [33]. In 2008, Blach et al. investigated the absorption capacities of several CDs aqueous solutions for toluene [34]. The absorption experiments showed that the studied CDs, including α-CD, β-CD and RAMEB, can significantly reduce the Henry's law constant of toluene. The most efficient absorbent is β-CD solution, which is 250 time more efficient than water. Moufawad et al. studied the ability of CDs to retain their host/guest properties in a commonly studied DES (choline chloride:urea 1:2) [35]. The researchers proved that the dissolution of β-CD in this DES is exothermic (enthalpy of dissolution of −23.3 J/g) and that the obtained supramolecular solvents can significantly decrease the volatility of four VOCs due to the formation of inclusion complexes. Four kinds of supramolecular DESs (SUPRADES), derived from modified CDs and levulinic acid, were used to absorb five VOCs [31]. The vapor–liquid partition coefficient value of toluene in RAMEB-based SUPRADES shows 250-fold reduction compared with its value in water. In addition, the percentage of dichloromethane (DCM) and toluene absorbed by SUPRADES reaches 95 % and 99 %, respectively. Recently, Triolo et al. systematically explored the aggregation state of CDs and molecular interactions in the SUPRADES heptakis-(2,6-di-O-methyl)-β-CD:levulinic acid 1:27 [32]. The results of X-ray scattering showed that CDs were homogeneously distributed in bulk. This phenomenon was further explained by molecular dynamic (MD) simulation, where the homogeneity of the system was maintained by hydrogen bonding (HB) interaction together with dispersive forces. Despite these scientific advances in the field of SUPRADES, research on VOCs absorption with SUPRADES is still insufficient and the microscopic absorption mechanism remains unexplored [35,36].

In this study, the effectiveness and molecular mechanisms of using SUPRADES as VOCs absorbents were systematically investigated. First, several SUPRADES were prepared from RAMEB and five types of HBDs. Then, the density and viscosity of these SUPRADES were determined from 293.15 K to 333.15 K. Six VOCs commonly found in biogas, including DCM, 1,2-dichloroethane (DCE), chloroform ($CHCl_3$), toluene, limonene and octamethylcyclotetrasiloxane (D_4), were chosen for the absorption experiments. The partition coefficient (P) together with absorption capacity of VOCs in RAMEB-based SUPRADES and corresponding pure HBDs were measured by static headspace-gas chromatography (SH-GC). The effects of some key factors, for example, VOC concentration in the gas phase, absorption temperature and water content of the SUPRADES, on the partition coefficients were discussed. Then, the regeneration performance of SUPRADES were evaluated by six absorption–desorption tests. Finally, the molecular phenomenon and the absorption mechanism were investigated by means of MD simulation.

2. Experimental section

2.1. Materials

Ethylene glycol (EG) (>99.5 %), 1,2-propanediol (PG) (>99 %), 1,3-butanediol (BUOL) (>99 %), triethylene glycol (TEG) (>99 %), benzyl alcohol (BA) (>99 %), dichloromethane (>99.95 %), 1,2-dichloroethane (>99.8 %), chloroform (>99.8 %), toluene (>99.8 %), limonene (>98 %), octamethylcyclotetrasiloxane (>98 %) and deionized water were used directly in the experiment without further purification. RAMEB (DS = 12.9, Figure S1) was purchased from Wacker Chemie (Lyon, France). The water content of the studied absorbents was measured three times by Karl Fischer titration (C20S KF Titrator). Table 1 summarizes the composition and water content of the SUPRADES and organic solvents used in the current study.

2.2. Preparation and characterization of the absorbents

Accurate amount of HBA and HBD were mixed together at a molar ratio of 1:40. Then the mixtures were stirred for 8 h at 343.15 K to obtain transparent homogeneous solutions. The density (ρ) and viscosity (μ) of SUPRADES and pure organic solvents were determined with an Anton Paar kinematic viscometer (SVM 3001).

2.3. Vapor-liquid partition coefficients

The equilibrium vapor–liquid partition coefficient (P) refers to the distribution ratio of a given solute in the gas phase and liquid phase at the equilibrium state [37]. As a commonly used thermodynamic parameter describing the vapor–liquid equilibrium, the P is of great importance for understanding the interaction between different molecules, which is defined as follows [38]

$$P = \frac{C_G}{C_L} \tag{1}$$

where C_G and C_L are mole concentration of solute in gas phase and liquid phase, respectively.

The phase ratio variation (PRV) method and the vapor phase calibration (VPC) method were used respectively to determine the P values of VOCs in water and other absorbents as described by Kolb and Ettre [39]. The detailed method for determining P values can be found in previous publications [18,37].

The measurement of P values at different temperatures was conducted on a Thermo Scientific TriPlusTM 500 headspace autosampler coupled to a Trace 1300 gas chromatograph (GC) equipped with a flame ionization detector and a DB 624 column. The column temperature of GC was set at 313.15, 353.15, 343.15, 353.15, 393.15 and 433.15 K for

Table 1
Composition and water content (mass fraction) of the SUPRADES and organic solvents for the current study.

Abbreviation	HBA	HBD	Molar ratio	Water content (%)
REG	RAMEB	Ethylene glycol	1:40	3.12
RPG	RAMEB	1,2-Propanediol	1:40	2.38
RBUOL	RAMEB	1,3-Butanediol	1:40	2.08
RTEG	RAMEB	Triethylene glycol	1:40	1.62
RBA	RAMEB	Benzyl alcohol	1:40	1.78
EG	–	Ethylene glycol	–	0.47
PG	–	1,2-Propanediol	–	0.52
BUOL	–	1,3-Butanediol	–	0.21
TEG	–	Triethylene glycol	–	0.22
BA	–	Benzyl alcohol	–	0.07

the detection of DCM, DCE, $CHCl_3$, toluene, limonene and D_4, respectively. Firstly, VOC stock solutions of known concentrations were injected into a 20 mL vial to which 3.5 g of absorbent had been previously added. Then, the vial was continuously stirred and equilibrated for 24 h before SH-GC analysis. The effect of VOC concentration, absorption temperature and water content of the absorbent on the *P* values was systematically investigated.

2.4. Formation constant

The formation constants (K_f) of three VOCs (DCE, limonene, D_4) with RAMEB were determined by SH-GC analysis. In the prepared samples, equal amounts of VOC were added to 20 mL vials containing 10 mL of water or RAMEB aqueous solutions at different concentrations. The vials were sealed and kept at 303.15 K. After 2 h of equilibration, an aliquot of the gas phase was taken and injected directly into the gas chromatograph. The formation constants were obtained from the chromatographic peak areas by using an algorithmic treatment [40].

2.5. Regeneration of the absorbents

The VOCs loaded DESs were uncapped and regenerated by stirring at 333.15 K for 12 h. Then they were analyzed by SH-GC to make sure that there were no VOC left in the DESs. The regenerated DESs were then used again to evaluate the *P* values and absorption ratio according to the same experimental procedure described above. Six absorption–desorption cycles were performed for five SUPRADES.

3. Calculation section

The Gaussian 09 (version D.01) software was employed on the geometry optimization of RAMEB at the level of m062x/6–311 + G^{**} and other molecules were optimized at ωB97XD/6–311++G^{**} level [41–43]. The restrained electrostatic potential (RESP) calculation was carried out on the popular Multiwfn 3.8 program to get atomic charges of molecules under studied (see Table S1) [44]. The MD simulations were then performed on GROMACS (version 2019.6) package [45]. The CHARMM36 force field was used to model RAMEB and the general AMBER force field was used for other molecules [46,47]. Additionally, the TIP3P potential was used to describe water for SUPRADES solutions [48]. The atomic labels and structures for different molecules were displayed in Figure S2.

The box size and composition of the three types of systems were listed in Table S2. The first type of system consists of pure solvent and is used to verify the accuracy of the simulation method. As shown in Table S3, the average relative deviation between experimental density and predicted results from simulation for eight solvents is 2.80 %, verifying the applicability of selected force field and simulation procedures to systems under study. The second type of system contains SUPRADES-$CHCl_3$ binary mixtures with different $CHCl_3$ concentrations to investigate the effect of VOC concentration and type of SUPRADES on absorption behavior. The last type of system was built to explore the effect of water content on the REG-$CHCl_3$ mixture. The detailed

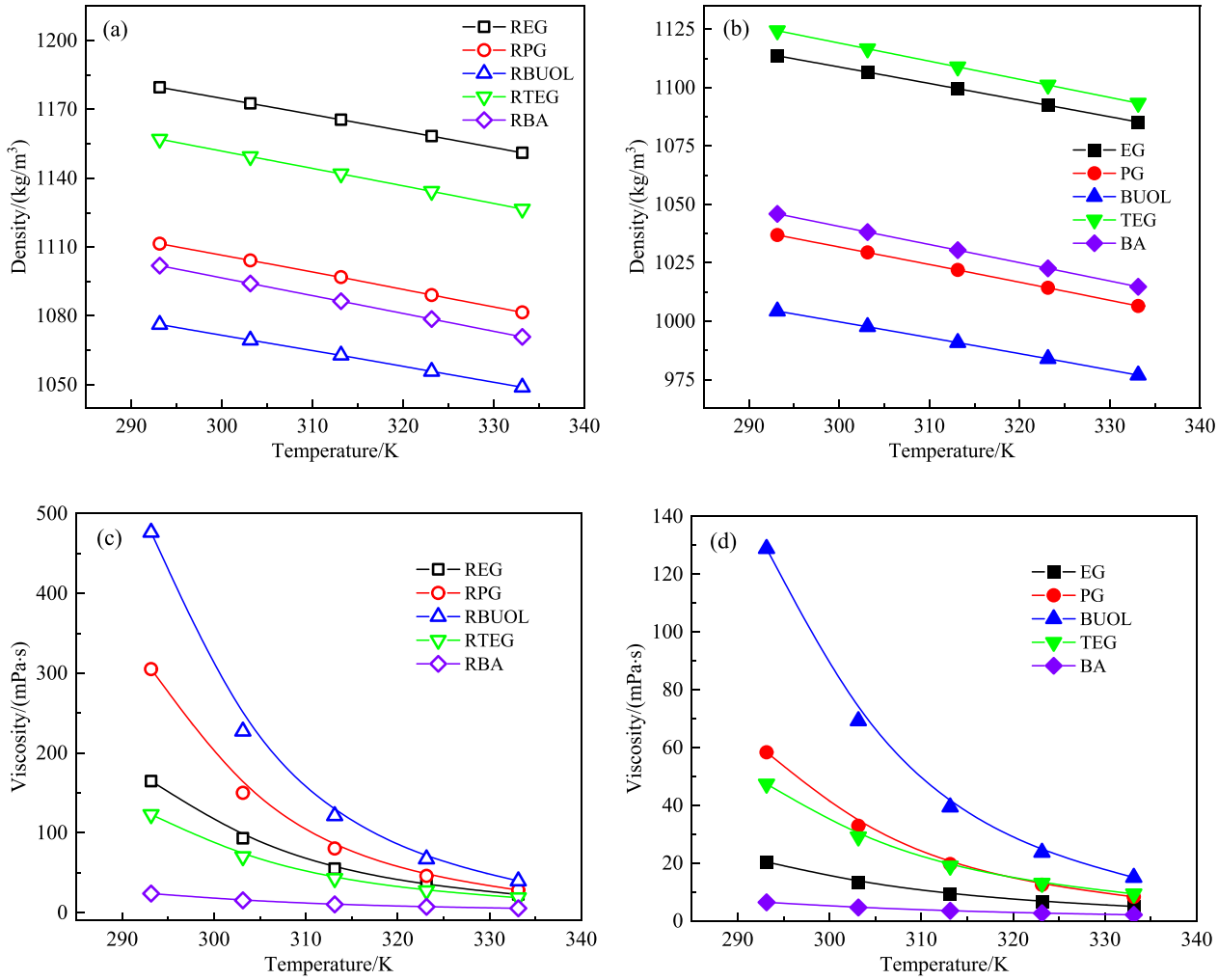

Fig. 1. Density of SUPRADES (a) and pure organic solvents (b); viscosity of SUPRADES (c) and organic solvents (d) at different temperatures. (Error < 1 %).

procedures of MD simulation are shown in Supporting Information Section 1.

4. Results and discussion

4.1. Density and viscosity of absorbents

The density and viscosity are important physical properties that affect mass transfer efficiency of VOCs in absorbents. Results obtained for SUPRADES and pure organic solvents are depicted in Fig. 1 as a function of temperature. Apparently, the density and viscosity of all solvents decrease with the increase of temperature. The effect of temperature changes on viscosity is more obvious than on density. For example, the viscosity of RBUOL at 333.15 K (39.71 mPa·s) is less than 9 % of that at 293.15 K (476.78 mPa·s), suggesting that the fluidity of the absorbent can be improved by increasing the absorption temperature. From the experimental data presented in Fig. 1(a) and (b), the density of SUPRADES is higher than that of the corresponding pure solvent at the same temperature, and this conclusion holds true for the viscosity. As can be seen in Fig. 1(a), REG has the highest density among the five SUPRADES, while RBUOL is just the opposite. For diols such as EG, PG and BUOL, the longer their carbon chain length, the lower the density and the greater the viscosity. The density and viscosity of SUPRADES based on diols also satisfy this law. Among the measured SUPRADES, RBA has the smallest viscosity, followed by RTEG, while the viscosity of REG (22.78 mPa·s) is close to that of RTEG (18.69 mPa·s) at 333.15 K. This result demonstrates that REG has good fluidity under appropriate absorption temperature.

4.2. VOCs absorption

The partition coefficients of DCM, DCE, $CHCl_3$, toluene, limonene, and D_4 in water, and in the studied absorbents at 303.15 K are listed in Table 2. The ratio of P_{water} to $P_{absorbent}$ (P_{ratio}) was also calculated to vividly demonstrate the absorption ability of different absorbers for VOCs.

It can be seen from Table 2 that the experimental P values of VOCs in water obtained in this study are close to that collected from literature, which verifies the reliability of the experimental device. The P values of 6 VOCs in SUPRADES and pure organic solvents are all much smaller than those determined in water, indicating that the chosen absorbents are more effective at absorbing VOCs than water. It can be observed that the P values of toluene, limonene and D_4 in water are much higher than those of the three chlorinated VOCs. It is worth noting that the hydrophobicity of limonene and D_4 is greater than that of toluene and of the three chlorinated VOCs, resulting in quite different P values in water. Directly affected by the difference in P value of VOCs in water, the P_{ratio} of VOCs in the same absorbent varies greatly. For highly hydrophobic VOCs such as limonene and D_4, the P_{ratio} for REG are above 300, but the P_{ratio} of DCM is only 8.5. Furthermore, P_{ratio} of the same VOC in different absorbents vary greatly due to different absorbent characteristics. Taking toluene as an example, the P_{ratio} of toluene in BA is almost 8 times that of EG due to the π-π interaction between toluene and BA [49]. EG with a shorter carbon chain is obviously not as effective as PG and BUOL in absorbing VOCs, especially for VOCs with large molecular volume (limonene and D_4).

One of the main purposes of this study is to investigate whether SUPRADES improve the VOCs absorption ability of the corresponding pure organic solvents. Except for D_4, the P values of the other five VOCs in two diol-based SUPRADES (RPG, RBUOL) are significantly smaller than those in their corresponding pure diols. Interestingly, the obtained P values of all 6 VOCs in REG are smaller than those in EG. In particular, the P values of $CHCl_3$ and limonene in EG are the largest among the five pure solvents. However, the P values of these two VOCs in REG are the smallest among the absorbents studied. This finding highlighted the improvement of VOCs absorption ability by combining RAMEB and organic solvents. For RTEG and RBA a different phenomenon was observed, that is, the P values in the two SUPRADES are close to the P values in the corresponding pure solvents. BA shows the greatest ability to solubilize DCE, toluene and D_4 compared to the other solvents, and considering its good fluidity (see Fig. 1(c)), it is a promising absorbent for VOCs removal.

The experimental results presented so far suggest that the combination of RAMEB and EG shows better VOCs absorption performance than pure EG, making REG even the most efficient absorbent for the capture of $CHCl_3$ and limonene.

4.3. Determination of formation constant

The formation constant is a type of equilibrium constant that describes the formation of an inclusion complex from a host molecule and a guest molecule. To investigate the ability of RAMEB to encapsulate and solubilize VOCs in depth, the formation constants of the RAMEB/VOC inclusion complexes were measured in water at 303.15 K [40].

For the three chlorinated VOCs, the formation constant follows this sequence $CHCl_3$ (93 M^{-1}) > DCE (43 M^{-1}) > DCM (12 M^{-1}),

Table 2
Partition coefficients (P) for DCM, DCE, $CHCl_3$, toluene, limonene, and D_4 in water, and in the studied absorbents at 303.15 K. (Error < 5 %).

Absorbent	DCM	P_{ratio}	DCE	P_{ratio}	$CHCl_3$	P_{ratio}	toluene	P_{ratio}	limonene	P_{ratio}	D_4	P_{ratio}
Water	1.1E-01		6.4E-02		1.7E-01		2.8E-01		1.8		5.7	
	1.4E-01[a]		4.8E-02[b] (298.15 K)		1.5E-01[c] (297.95 K)		2.5E-01[a]		1.9[d]		4.0[c]	
	9.0E-02[c] (297.95 K)						2.9E-01[e]		2.3[e]		5.0[f] (293.15 K)	
REG	1.3E-02	8.5	3.0E-03	21.3	1.8E-03	94.4	2.3E-03	121.7	2.0E-04	8750.0	1.5E-02	380.0
RPG	1.1E-02	10.0	3.4E-03	18.8	2.9E-03	58.6	2.5E-03	112.0	3.9E-04	4487.2	9.1E-03	626.4
RBUOL	3.3E-03	33.3	4.1E-03	15.6	3.4E-03	50.0	3.9E-03	71.8	5.1E-04	3431.4	1.0E-02	570.0
RTEG	8.0E-03	13.8	2.0E-03	32.0	2.3E-03	73.9	2.2E-03	127.3	5.0E-04	3500.0	1.4E-02	407.1
RBA	8.8E-03	12.5	1.8E-03	35.6	3.1E-03	54.8	1.3E-03	215.4	2.7E-04	6481.5	1.4E-03	4071.4
EG	2.1E-02	5.2	7.1E-03	9.0	9.0E-03	18.9	9.1E-03	30.8	6.2E-03	282.3	4.0E-02	142.5
PG	1.3E-02	8.5	4.7E-03	13.6	3.9E-03	43.6	4.1E-03	68.3	1.3E-03	1346.2	7.0E-03	814.3
BUOL	1.3E-02	8.5	4.8E-03	13.3	4.7E-03	36.2	3.3E-03	84.8	1.0E-03	1750.0	7.4E-03	770.3
TEG	7.0E-03	15.7	1.9E-03	33.7	2.4E-03	70.8	2.5E-03	112.0	1.4E-03	1250.0	1.2E-02	475.0
BA	6.9E-03	15.9	1.7E-03	37.6	3.6E-03	47.2	1.1E-03	254.5	2.3E-04	7608.7	8.3E-04	6867.5

[a] ref [31],
[b] ref [50],
[c] ref [51],
[d] ref [52],
[e] ref [18],
[f] ref [53].

demonstrating that the strength of the interaction between RAMEB and $CHCl_3$ to form an inclusion complex is stronger than that of the other two chlorinated VOCs [54]. The formation constants of toluene and limonene with RAMEB are 238 and 2716 M^{-1}, respectively. The high formation constant obtained for RAMEB/limonene reflects the excellent complexing ability of RAMEB with limonene. Although D_4 is a hydrophobic VOC like toluene and limonene, the formation constant of D_4 is only 8 M^{-1} [34]. This is in good agreement with the experimental results of the partition coefficients. As shown in Table 2, except for EG, the beneficial effect on D_4 absorption was not observed when RAMEB was added to pure solvents. This may be because the D_4 molecule is too large to form an inclusion complex with RAMEB.

4.4. Effect of VOC concentration

The concentration of VOCs in the gas phase is a critical factor that affects the absorption capacity (mg VOC/ g absorbent) and the absorption ratio of the absorbent. The absorption ratio (*AR*) of absorbent is calculated by eq. (2).

$$AR = \left(1 - \frac{m_{absb}}{m_{feed}}\right) \times 100\% \quad (2)$$

where m_{absb} and m_{feed} are the mass of VOC absorbed in the solvent at equilibrium state and the mass of VOC in the feed, respectively.

As we can see in Fig. 2(a), the absorption capacity of REG and EG increases almost linearly as DCM concentration increases. It is quite obvious that the absorption capacity of REG is higher than that of EG under the same DCM concentration. The similar advantage of REG over EG was observed for absorption ratio (see Fig. 2(b)). This observation is consistent with the partition coefficient results, suggesting that REG exhibited better performance in absorbing DCM than EG. It is worth noting that the *AR* of REG fluctuates around 94 % as the DCM concentration increases, while for EG, *AR* is about 91 %.

4.5. Effect of temperature

The effect of temperature on the DCM partition coefficient was studied at 303.15 K, 318.15 K and 333.15 K. As depicted in Fig. 3, the partition coefficient of DCM is strongly impacted by the temperature. For all absorbents, *P* values increase with the increase of temperature. Take REG for example, the *P* value of DCM is 1.3E-2 at 303.15 K, while it increases to 2.4E-2 at 333.15 K. This means that lowering the absorption temperature can be an effective approach to improve the absorption capacity of absorbent for VOCs. It should be noted that lowering the temperature will increase the viscosity of the solvent, thereby hindering the mass transfer of the system. Therefore, both partition coefficient and viscosity should be taken into consideration when optimizing the absorption temperature.

4.6. Effect of water content

Since both the feed gas and the air inevitably contain moisture, the effect of water on the VOCs capture performance of the absorbent cannot be ignored. Fig. 4 shows the effect of REG water content on the partition coefficient of 6 VOCs at 303.15 K. When water content increases from 20 wt% to 80 wt%, the partition coefficients of all VOCs increase significantly. A case in point is the absorption of toluene, where the *P* value is only 3.6E-03 at a water content of 20 wt%, while this value increases by a factor of 6.5 at a water content of 80 wt%. This indicates that the addition of water negatively affects the absorption capacity of VOCs by REG. In addition, higher water content increases the energy consumption of absorbent recovery due to the high heat capacity of water. The positive effect of adding water is to reduce solvent viscosity and reduce solvent costs, as in the case of CO_2 capture process with ethanolamine solution. Therefore, water content should be evaluated comprehensively by taking both positive and negative effects into account.

4.7. Regeneration of absorbents

Absorbent regeneration is a critical part of the VOC removal process. In particular, the ease of recovery, the energy consumption and the physicochemical stability of absorbent after desorption have always been topics of concern. In this study, a simple heating and stirring method was used to regenerate the five SUPRADES. Fig. 5 (a) and (b) show the effect of recycle time on the P_{ratio} and absorption ratio of $CHCl_3$, respectively. For all absorbents under study, no negative effects on P_{ratio} and absorption ratio were observed from the increase in the regeneration time. In particular, the absorption ratio of REG in the six absorption–desorption cycles was maintained at about 99 %, which highlights its high efficiency and stability in absorbing $CHCl_3$.

4.8. Results of MD simulation

4.8.1. Structure of SUPRADES

It is necessary to study the molecular structure of SUPRADES, because this determines whether the absorbent remains stable. An interesting study by Triolo et al. reported that β-CD could dissolve in DES (choline chloride:urea 1:2), without aggregation phenomena [55].

In this study, a representative snapshot of RAMEB – EG system at 303.15 K is shown in Figure S3, where RAMEB is homogeneous distributed in the EG matrix. This phenomenon suggests that RAMEB

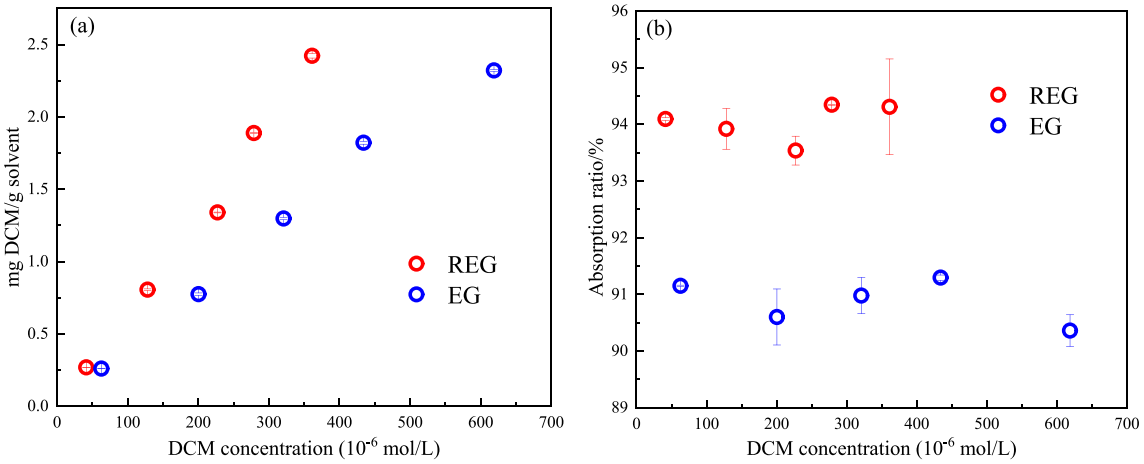

Fig. 2. Effect of concentration of DCM in the gas phase on the absorption capacity (a) and absorption ratio (b) at 303.15 K.

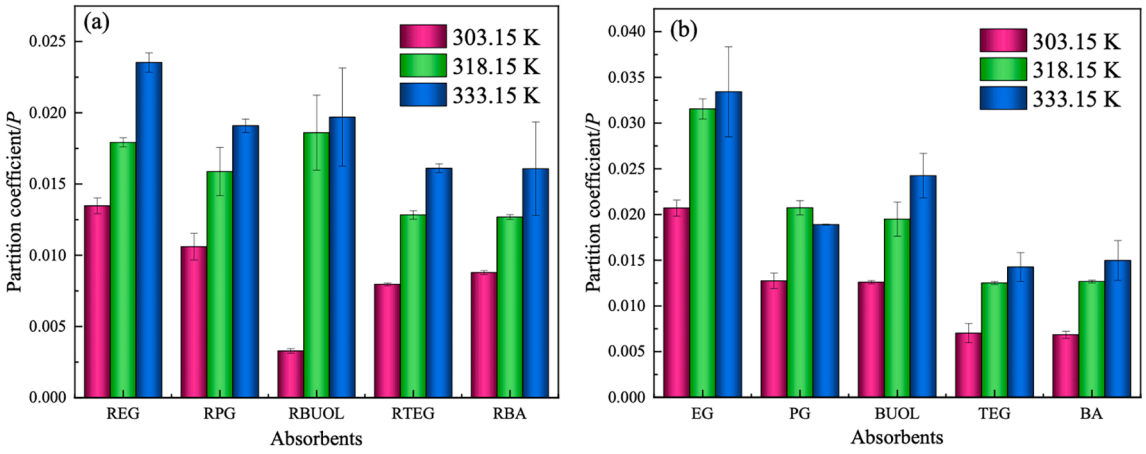

Fig. 3. Effect of absorption temperature on the DCM partition coefficient of SUPRADES (a) and pure organic solvents (b).

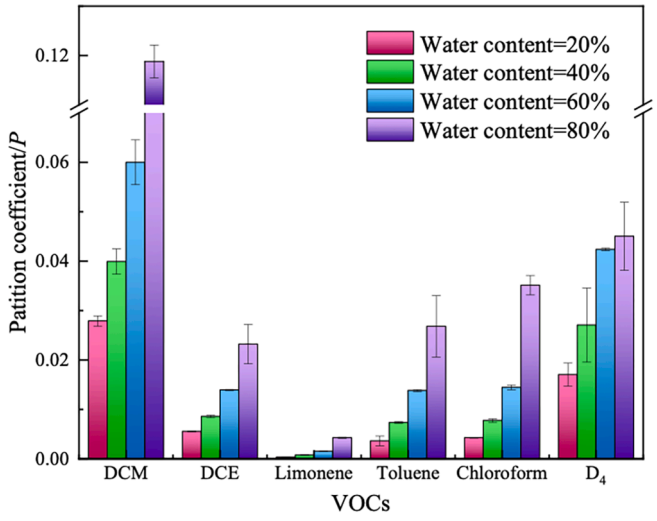

Fig. 4. Effect of water content (mass fraction) of REG on the partition coefficient (*P*) for different VOCs at 303.15 K.

can form stable and homogeneous solvent with EG. To further explain the formation of REG and explore the effect of water on REG, the average number of HB count per RAMEB in pure REG and water-containing REG was depicted in Fig. 6. For pure REG, each RAMEB molecule forms an average of six HBs with EG, hindering the aggregation of neighbor CDs. The addition of water has almost no effect on the HBs in RAMEB molecules, which is one of the guarantees to maintain the structure stability of the CD molecule. However, as the water content in REG increases, the number of HBs between RAMEB and EG decreases sharply, while the number of HBs between RAMEB and water gradually increase. The HBA and HBD of RAMEB originally occupied by EG gradually combine with water molecules, resulting in the destruction of the original HB network of REG.

4.8.2. *Interaction energy analysis*

To determine the strength and type of interaction between key components of the absorbent and $CHCl_3$, the interaction energy analysis was carried out for various $CHCl_3$-containing systems. The total interaction energy (E_{total}) consists of two parts: electrostatic energy (E_{ele}) and van der Waals energy (E_{vdW}).

Table 3 shows the influence of absorbent type on the interaction energy. For all solvents, E_{vdW} dominates the interaction energy with $CHCl_3$. Especially for the three SUPRADES, the magnitude of E_{vdW} is approximately five times that of E_{ele}. This means that van der Waals force contributes the most to the absorption of $CHCl_3$. The magnitude of

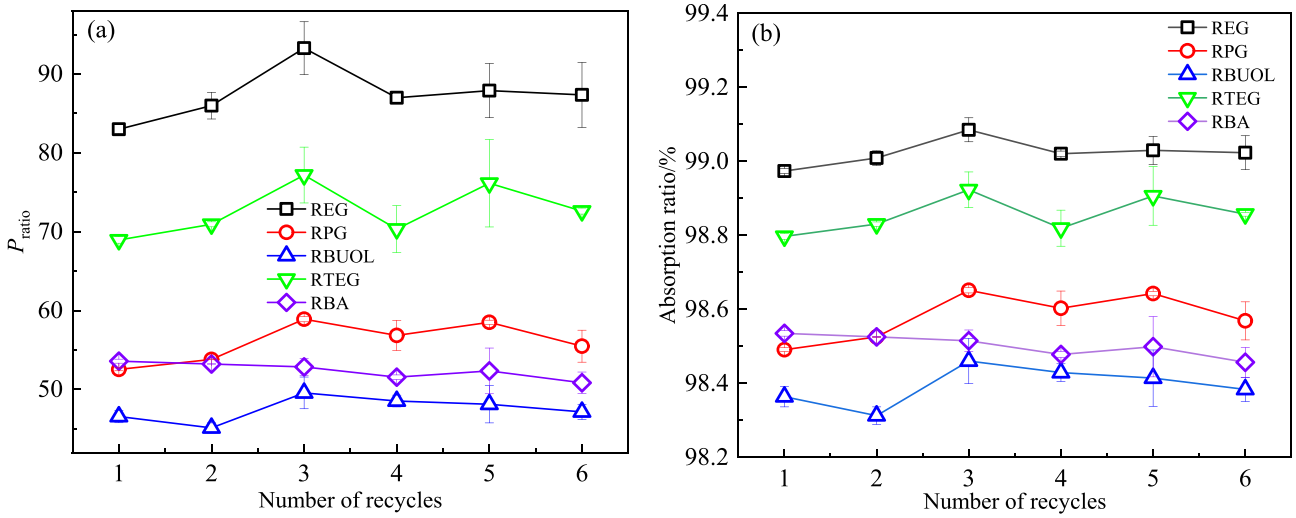

Fig. 5. Effect of SUPRADES recycle times on the ratio of partition coefficient of $CHCl_3$ in water to that in SUPRADES (P_{ratio}) (a); on the absorption ratio of $CHCl_3$(b).

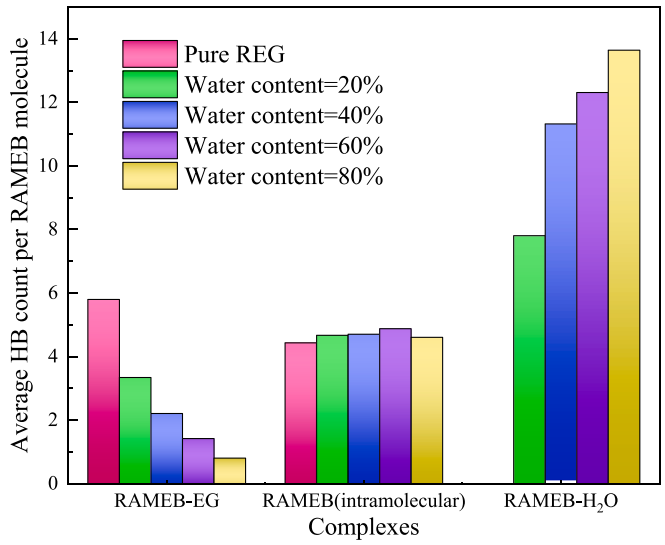

Fig. 6. Effect of water content on the average HB count per RAMEB molecule in RAMEB-EG, RAMEB (intramolecular) and RAMEB-H_2O.

Table 3
The interaction energy of H_2O – / HBD – / HBA – / absorbent – $CHCl_3$ in four $CHCl_3$-containing systems (mass fraction of $CHCl_3$ = 7 %).

Solvents		E_{ele}/(kJ/mol)	E_{vdW}/(kJ/mol)	E_{total}/(kJ/mol)
Pure water	H_2O – $CHCl_3$	−6.58	−18.06	−24.65
REG – $CHCl_3$	RAMEB – $CHCl_3$	−3.45	−22.31	−25.76
	EG – $CHCl_3$	−8.00	−33.37	−41.37
	Absorbent – $CHCl_3$	−11.45	−55.68	−67.13
RPG – $CHCl_3$	RAMEB – $CHCl_3$	−3.00	−14.58	−17.58
	PG – $CHCl_3$	−8.38	−38.44	−46.82
	Absorbent – $CHCl_3$	−11.38	−53.02	−64.40
RBUOL – $CHCl_3$	RAMEB – $CHCl_3$	−2.21	−13.21	−15.42
	BUOL – $CHCl_3$	−7.42	−40.28	−47.70
	Absorbent – $CHCl_3$	−9.63	−53.49	−63.12

interaction energy between the four absorbents and $CHCl_3$ follows this order: REG (67.13 kJ/mol) > RPG (64.40 kJ/mol) > RBUOL (63.12 kJ/mol) > H_2O (24.65 kJ/mol). This result is consistent with the experimental partition coefficients from Table 2, that is, REG (1.8E-03) < RPG (2.9E-03) < RBUOL (3.4E-03) < H_2O (1.7E-01). Although the molar ratio between RAMEB and EG is 1:40, the interaction energy between RAMEB and $CHCl_3$ still exceeds 38 % of the total interaction energy, reflecting the important role of CD in $CHCl_3$ absorption.

Fig. 7 displays the effect of three different $CHCl_3$ concentration (1.5 %, 7 % and 13.5 %) on the interaction energy. When the mass of the absorbent remains constant, the total interaction energy between the absorbent and $CHCl_3$ decreases as the amount of $CHCl_3$ increases (see Fig. 7 (a)). This downward trend is more pronounced for water, possibly due to the very limited absorption capacity of water for $CHCl_3$. As can be seen from Fig. 7(b), the increase in $CHCl_3$ content weakens the interaction strength between RAMEB and diol, probably because the potential binding sites between the key components of SUPRADES are gradually occupied by $CHCl_3$ molecules. In addition, the electrostatic energy between RAMEB and diol is slightly smaller than the van der Waals energy. Considering that six effective HBs were formed between RAMEB and EG shown in Fig. 6, and HB belongs to the E_{ele}, this phenomenon further illustrates the important contribution of HB to the formation of SUPRADES.

4.8.3. Self-diffusion coefficients

As one of the most difficult transport coefficients to measure experimentally, the self-diffusion coefficient (*D*) is an important index to evaluate the dynamic property of absorbents [56]. Fortunately, GROMACS provides a natural and convenient alternative to the calculation of self-diffusion coefficient. The *D* value of $CHCl_3$, diols and RAMEB in nine different systems were calculated by MD method at 303.15 K. As shown in Fig. 8 (a), the *D* values of $CHCl_3$ and diols for REG and RPG systems increase with the increase of CH_3Cl concentration. This may be because the increased concentration of CH_3Cl improves the fluidity of these systems. The self-diffusion coefficient shows different patterns in the RBUOL system. When the CH_3Cl concentration increases from 1.5 to 7 %, the *D* value of $CHCl_3$ and BUOL increases, but when the CH_3Cl concentration continues to increase to 13.5 %, the *D* value slightly decreases.

Additionally, under the same concentration of CH_3Cl, the magnitude of *D* of $CHCl_3$ in different diol systems follows this sequence *D* (REG) > *D*

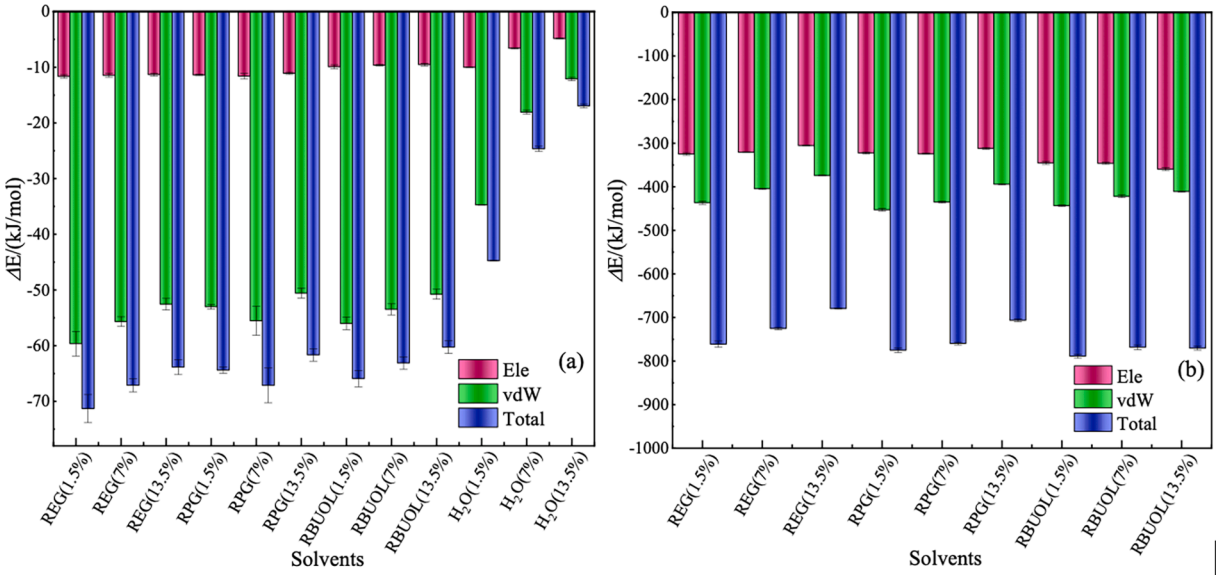

Fig. 7. Effect of $CHCl_3$ concentration on the interaction energy between absorbent and $CHCl_3$ (a); on the interaction energy between diol and RAMEB(b). Mass fraction of $CHCl_3$ in these systems are 1.5%, 7% and 13.5%, respectively.

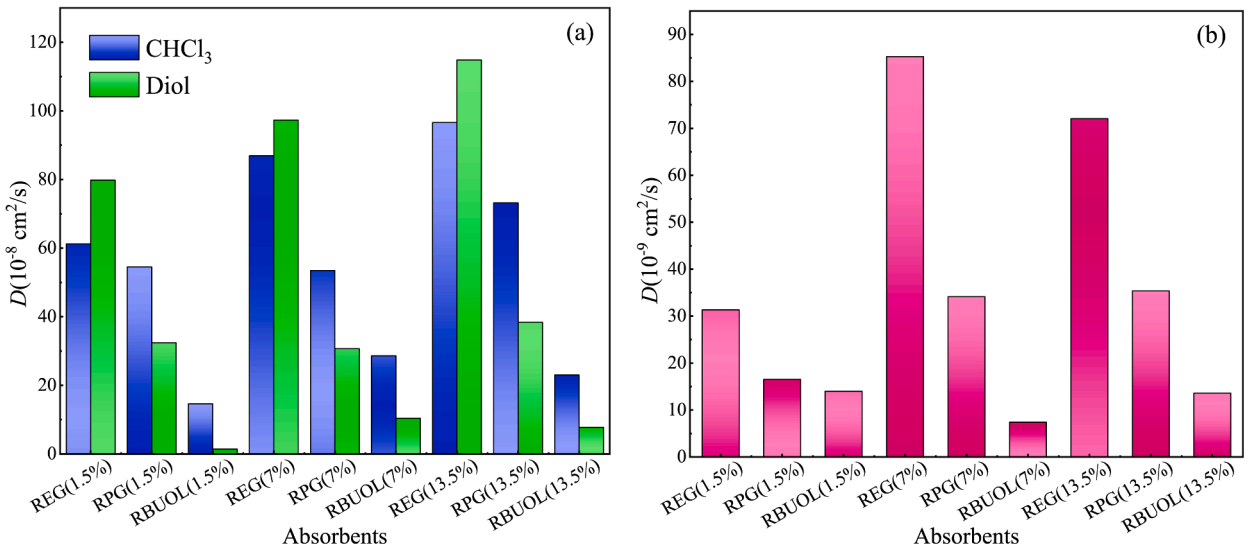

Fig. 8. Self-diffusion coefficients (D) of $CHCl_3$, diols (a) and RAMEB (b) in nine systems at 303.15 K. Mass fraction of $CHCl_3$ in three systems are 1.5 %, 7 % and 13.5 %, respectively.

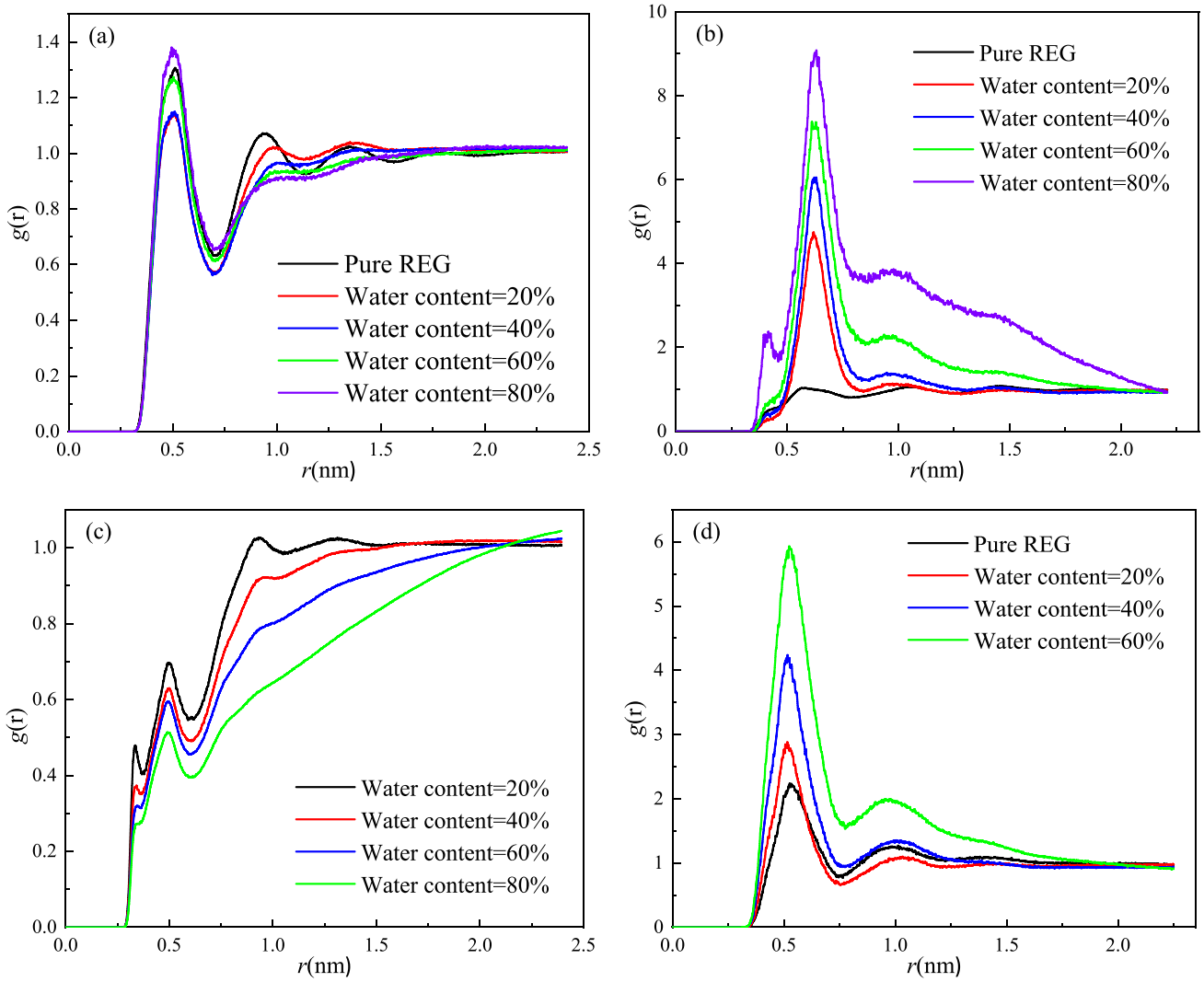

Fig. 9. RDFs for C1 of $CHCl_3$ – C1 of EG (a); C1 of $CHCl_3$ – C2 of RAMEB (b); C1 of $CHCl_3$ – O1 of H_2O (c); C1 of $CHCl_3$ – $CHCl_3$ (d) for different water containing REG – $CHCl_3$ systems. Mass fraction of $CHCl_3$ is 7.0%.

(RPG) > *D* (RBUOL), which is consistent with the results of SUPRADES viscosity shown in Fig. 1 (c). Therefore, the long alkyl chain of diol decreases the *D* value and increases the viscosity of the diol. This phenomenon demonstrates that the diffusion of CH_3Cl in the REG is faster than that in RPG and RBUOL. It should be noted that the *D* value of diol and $CHCl_3$ is larger than that of RAMEB, owing to the large molecular size of RAMEB that hinders its diffusion. In short, among the three diol-based SUPRADES, REG provides the most favorable diffusion environment for $CHCl_3$.

4.8.4. Radial distribution function (RDF) analysis

The radial distribution function is an important structural characteristic that describes the average structure of systems at molecular length scale, especially for disordered molecular systems such as liquids [57,58]. The RDF profiles for different water containing REG – $CHCl_3$ systems are given in Fig. 9.

Fig. 9 (a) shows the effect of water content on the RDF profiles for C1 of $CHCl_3$ – C1 of EG. For five systems, the first sharp peak appears at about r = 0.51 nm, and the corresponding g(r) is not significantly affected by water content. However, the second peak of system without water is located at about 0.94 nm, which is stronger and closer than other water-containing systems. In addition, as the water content increases, the second peak becomes weaker. This means that the addition of water increases the separation distance between C1 of $CHCl_3$ and C1 of EG, and the interaction between EG and $CHCl_3$ is weakened by water. In Fig. 9 (b), the first strong peak of system without water appears at about 0.58 nm with g(r) value of 1.04, which is far smaller than that of other water-containing systems. The different effects of water on the RDF between EG – $CHCl_3$ and RAMEB – $CHCl_3$ may be due to the fact that EG is miscible with water, while RAMEB is only partially miscible with water. When water is added to the REG – $CHCl_3$ system, the water destroys the original structure of SUPRADES and drives more slightly water-soluble $CHCl_3$ molecules to concentrate around RAMEB molecules.

As shown in Fig. 9(c), the first two peaks for four water-containing systems are near 0.34 nm and 0.50 nm, respectively. The g(r) values of both peaks decrease with increasing water content. This phenomenon suggests that increasing water content weakens the interaction between water and $CHCl_3$. It can be seen from Fig. 9(d) that the strong peak of C1 of $CHCl_3$ – $CHCl_3$ is located at around 0.53 nm, while the separation distance for other water-containing systems are shorter and the peak are stronger. This result indicates that, adding water to the REG – $CHCl_3$ system promotes the aggregation of $CHCl_3$ molecules.

4.8.5. Spatial distribution function (SDF) analysis

Spatial distribution function is a 3-dimensional distribution of a molecule (or of an atom of a particle) in local coordinate system around a tagged one [59,60]. The distribution and interaction areas of molecules in the system can be vividly displayed through SDF analysis.

The SDFs of RAMEB – EG – $CHCl_3$ and RAMEB – PG – $CHCl_3$ systems are presented in Fig. 10. It is interesting to note that the RAMEB molecule embraces green isosurface which represents $CHCl_3$ molecule (see Fig. 10(a)). This inclusion phenomenon is further verified by the Figure S4, where some $CHCl_3$ molecules are located in the cavity of CD molecules. These observations could explain why the *P* value of $CHCl_3$ is lower in REG than in EG. That is, CD promotes the absorption of $CHCl_3$ by forming inclusion complexes with $CHCl_3$. Similarly, for the RAMEB-PG-$CHCl_3$ system, there is a green isosurface in the center of CD molecule, indicating the encapsulation of $CHCl_3$ by the CD (see Fig. 10(b)). As shown in Fig. 10(c), the EG molecule is surrounded by cage-shaped

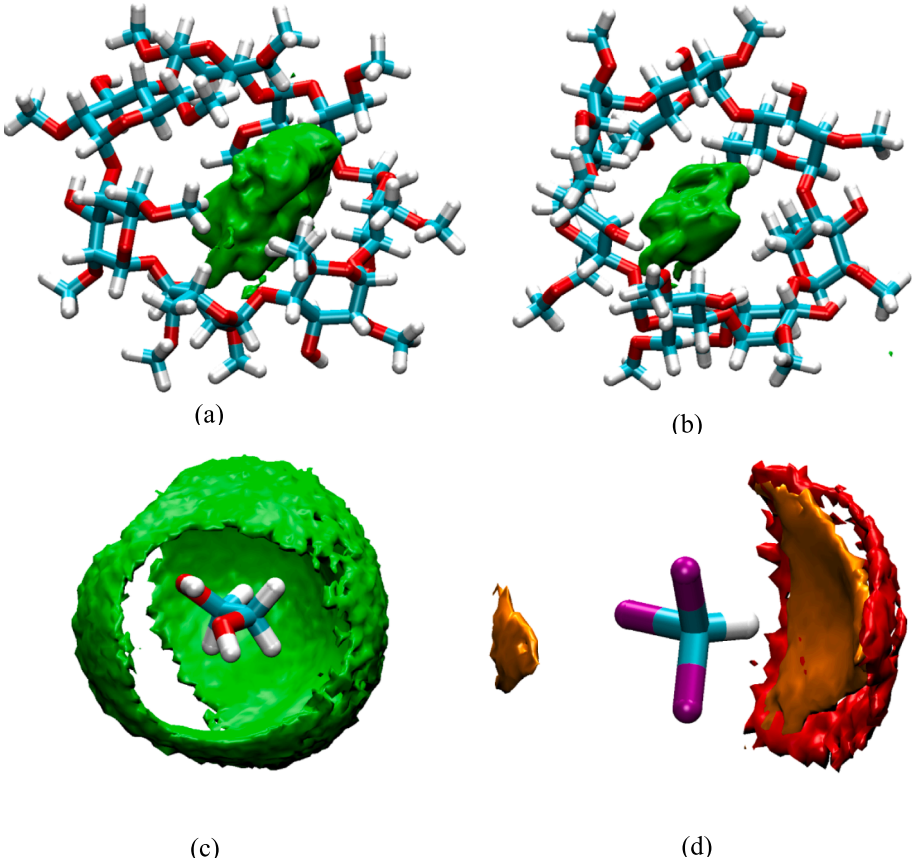

Fig. 10. SDFs of RAMEB – EG – $CHCl_3$ and RAMEB – PG – $CHCl_3$ systems, where mass fraction of $CHCl_3$ is 7.0%. SDFs of $CHCl_3$ around RAMEB in RAMEB – EG system (a); $CHCl_3$ around RAMEB in RAMEB – PG system (b); $CHCl_3$ around EG (c); RAMEB and EG around $CHCl_3$ (d). Orange isosurface: EG; green: $CHCl_3$; red: RAMEB. (For interpretation of the references to colour in this figure legend, the reader is referred to the web version of this article.)

green isosurface, but there is no green isosurface opposite the hydrogen atom of the hydroxyl group. Opposite the oxygen atoms of the two hydroxyl groups of the EG molecule, there is a strip-shaped isosurface, indicating that there may be C-H···O interaction between EG and $CHCl_3$. This speculation is also supported by phenomenon in Fig. 10(d), where a large orange isosurface is located opposite the hydrogen atoms of $CHCl_3$ and only a small isosurface is opposite the chlorine atoms. There are some sparse red isosurfaces behind the orange isosurface, demonstrating that the separation distance between EG and $CHCl_3$ is shorter than that between CD and $CHCl_3$. All large isosurfaces are on the hydrogen side of $CHCl_3$, illustrating that $CHCl_3$ molecule tends to interact with REG through its hydrogen atom.

5. Conclusion

In this study, the strategy of VOCs absorption using new SUPRADES was systematically evaluated from vapor-liquid experiment to MD simulation. The density and viscosity of prepared SUPRADES and organic solvents were measured experimentally and compared. The results suggest that REG, RTEG and RBA have good fluidity. The partition coefficients data of six VOCs in water, SUPRADES and organic solvents were obtained by SH-GC analysis. It was found that *P* values of most VOCs in three diol-based SUPRADES (*i.e.,* REG, RPG, RBUOL) are significantly smaller than those in their corresponding diols. Especially, the combination of RAMEB and EG significantly improves the absorption ability of EG, even making REG the most efficient absorbent for the capture of $CHCl_3$ and limonene.

The obtained formation constants for RAMEB/VOCs inclusion complexes in water demonstrate that the interaction between RAMEB and $CHCl_3$ is stronger than that of DCM and DCE. Besides, the high formation constant of RAMEB/limonene (2716 M^{-1}) reflects the excellent complexation ability of RAMEB with limonene. By studying key factors affecting the absorption process, we found that increasing the concentration of VOCs in the gas phase, lowering the absorption temperature and reducing the water content can be effective ways to reduce the *P* value of VOCs in absorbents. The regeneration test shows that the $CHCl_3$ absorption ratio of REG was maintained around 99 %, highlighting its high absorption efficiency and stability.

The molecular insights into the relationship between SUPRADES structures and absorption behavior was obtained from MD simulation. The HBs between CD and EG hinders the aggregation of neighbor CDs, helping CDs form stable and homogeneous solvent with EG. The interaction energy analysis demonstrates that van der Waals force contributes the most to the absorption of $CHCl_3$ by REG. The result of self-diffusion coefficient shows that REG provides the most favorable diffusion environment for $CHCl_3$ compared with RPG and RBUOL, which is consistent with viscosity data. Finally, the RDF analysis was used to vividly displayed the 2-dimensional molecule distribution of SUPRADES systems and SDF analysis verifies the formation of RAMEB-$CHCl_3$ inclusion complexes in absorption process.

All in all, we have clearly demonstrated that some SUPRADES, composed of RAMEB and diols (*i.e.,* EG, PG), can be high-performance solvents for VOCs absorption. It should be noted that this study may provide new insights into understanding the physical absorption of various gases (*i.e.,* SO_2, CO_2) in SUPRADES, not limited to VOCs.

CRediT authorship contribution statement

Chengmin Gui: Writing – original draft, Data curation, Conceptualization. **Pedro Villarim:** Validation, Investigation. **Zhigang Lei:** Visualization, Supervision. **Sophie Fourmentin:** Writing – review & editing, Supervision, Resources, Methodology.

Declaration of competing interest

The authors declare that they have no known competing financial interests or personal relationships that could have appeared to influence the work reported in this paper.

Data availability

Data will be made available on request.

Acknowledgments

Chengmin Gui acknowledges the grant of China Scholarship Council. Pedro Villarim acknowledges, Région Hauts-de-France, "Dunkerque, l'Energie Créative" program and Starklab for the financial support of his PhD.

Appendix A. Supplementary data

Supplementary data to this article can be found online at https://doi.org/10.1016/j.cej.2024.148708.

References

[1] C.C. Chen, Y.H. Huang, J.Y. Fang, Hydrophobic deep eutectic solvents as green absorbents for hydrophilic VOC elimination, J. Hazard. Mater. 424 (2022), https://doi.org/10.1016/j.jhazmat.2021.127366.
[2] Y. Mu, P.T. Williams, Recent advances in the abatement of volatile organic compounds (VOCs) and chlorinated-VOCs by non-thermal plasma technology: A review, Chemosphere 308 (2022), https://doi.org/10.1016/j.chemosphere.2022.136481.
[3] G. Yu, N.F. Gajardo-Parra, M. Chen, B. Chen, G. Sadowski, C. Held, Aromatic volatile organic compounds absorption with phenyl-based deep eutectic solvents: A molecular thermodynamics and dynamics study, AIChE J 69 (2023), https://doi.org/10.1002/aic.18053.
[4] X. Li, L. Zhang, Z. Yang, P. Wang, Y. Yan, J. Ran, Adsorption materials for volatile organic compounds (VOCs) and the key factors for VOCs adsorption process: A review, Sep. Purif. Technol. 235 (2020), https://doi.org/10.1016/j.seppur.2019.116213.
[5] M. Song, K. Kim, C. Cho, D. Kim, Reduction of volatile organic compounds (Vocs) emissions from laundry dry-cleaning by an integrated treatment process of condensation and adsorption, Processes. 9 (2021), https://doi.org/10.3390/pr9091658.
[6] Z. Li, J. Liu, B. Gao, L. Bo, Cu-Mn-CeOx loaded ceramic catalyst for non-thermal sterilization and microwave thermal catalysis of VOCs degradation, Chem. Eng. J. 442 (2022), https://doi.org/10.1016/j.cej.2022.136288.
[7] C. Gui, R. Zhu, G. Li, C. Dai, G. Yu, Z. Lei, Natural Gas Dehydration with Ionic-Liquid-Based Mixed Solvents, ACS Sustain. Chem. Eng. 9 (2021) 6033–6047, https://doi.org/10.1021/acssuschemeng.1c01240.
[8] Y.S. Sistla, A. Khanna, CO2 absorption studies in amino acid-anion based ionic liquids, Chem. Eng. J. 273 (2015) 268–276, https://doi.org/10.1016/j.cej.2014.09.043.
[9] X. Zhang, B. Gao, A.E. Creamer, C. Cao, Y. Li, Adsorption of VOCs onto engineered carbon materials: A review, J. Hazard. Mater. 338 (2017) 102–123, https://doi.org/10.1016/j.jhazmat.2017.05.013.
[10] L. Zhu, D. Shen, K.H. Luo, A critical review on VOCs adsorption by different porous materials: Species, mechanisms and modification methods, J. Hazard. Mater. 389 (2020), https://doi.org/10.1016/j.jhazmat.2020.122102.
[11] R.J. Davis, R.F. Zeiss, Cryogenic condensation: A cost-effective technology for controlling VOC emissions, Environ. Progress. 21 (2002) 111–115, https://doi.org/10.1002/ep.670210213.
[12] V.K. Gupta, N. Verma, Removal of volatile organic compounds by cryogenic condensation followed by adsorption, 2002. www.elsevier.com/locate/ces.
[13] K. Everaert, J. Baeyens, Catalytic combustion of volatile organic compounds, J. Hazard. Mater. 109 (2004) 113–139, https://doi.org/10.1016/j.jhazmat.2004.03.019.
[14] F. Lin, Z. Zhang, N. Li, B.B. Yan, C. He, Z. Hao, G. Chen, How to achieve complete elimination of Cl-VOCs: A critical review on byproducts formation and inhibition strategies during catalytic oxidation, Chem. Eng. J. 404 (2021), https://doi.org/10.1016/j.cej.2020.126534.
[15] G. Li, K. Chen, Z. Lei, Z. Wei, Condensable gases capture with ionic liquids, Chem. Rev. (2023), https://doi.org/10.1021/acs.chemrev.3c00175.
[16] X. Ma, W. Wang, C. Sun, J. Sun, Comprehensive evaluation of ionic liquid [Bmim][PF6] for absorbing toluene and acetone, Environ. Pollut. 285 (2021), https://doi.org/10.1016/j.envpol.2021.117675.
[17] Y. Song, S. Chen, F. Luo, L. Sun, Absorption of toluene using deep eutectic solvents: quantum chemical calculations and experimental investigation, Ind. Eng. Chem. Res. 59 (2020) 22605–22618, https://doi.org/10.1021/acs.iecr.0c04986.
[18] P. Villarim, E. Genty, J. Zemmouri, S. Fourmentin, Deep eutectic solvents and conventional solvents as VOC absorbents for biogas upgrading: A comparative study, Chem. Eng. J. 446 (2022), https://doi.org/10.1016/j.cej.2022.136875.

[19] C. Gui, G. Li, Z. Lei, Z. Wei, Y. Dong, Experiment and molecular mechanism of two chlorinated volatile organic compounds in ionic liquids, Ind. Eng. Chem. Res. 62 (2023) 1160–1171, https://doi.org/10.1021/acs.iecr.2c04163.

[20] C.C. Chen, Y.H. Huang, S.M. Hung, C. Chen, C.W. Lin, H.H. Yang, Hydrophobic deep eutectic solvents as attractive media for low-concentration hydrophobic VOC capture, Chem. Eng. J. 424 (2021), https://doi.org/10.1016/j.cej.2021.130420.

[21] F.M. Perna, P. Vitale, V. Capriati, Deep eutectic solvents and their applications as green solvents, Curr. Opin. Green Sustain. 21 (2020) 27–33, https://doi.org/10.1016/j.cogsc.2019.09.004.

[22] P. Makoś-Chełstowska, VOCs absorption from gas streams using deep eutectic solvents – A review, J. Hazard. Mater. 448 (2023) 130957, https://doi.org/10.1016/j.jhazmat.2023.130957.

[23] P. Makoś-Chełstowska, E. Słupek, J. Gębicki, Deep eutectic solvent-based green absorbents for the effective removal of volatile organochlorine compounds from biogas, Green Chem. 23 (2021) 4814–4827, https://doi.org/10.1039/d1gc01735g.

[24] S. Indra, R. Subramanian, S. Daschakraborty, Absorption of volatile organic compounds toluene and acetaldehyde in choline chloride-based deep eutectic solvents, J. Phys. Chem. B 126 (2022) 3705–3716, https://doi.org/10.1021/acs.jpcb.2c00076.

[25] E. Supek, P. Makoś, J. Gębicki, A. Rogala, Purification of model biogas from toluene using deep eutectic solvents, in: E3S Web of Conferences, EDP Sciences, 2019. https://doi.org/10.1051/e3sconf/201911600078.

[26] P. Janicka, M. Kaykhaii, J. Płotka-Wasylka, J. Gębicki, Supramolecular deep eutectic solvents and their applications, Green Chem. 24 (2022) 5035–5045, https://doi.org/10.1039/d2gc00906d.

[27] H.M.C. Marques, A review on cyclodextrin encapsulation of essential oils and volatiles, Flavour. Frag. J. 25 (2010) 313–326, https://doi.org/10.1002/ffj.2019.

[28] M.E. Davis, M.E. Brewster, Cyclodextrin-based pharmaceutics: Past, present and future, Nat. Rev. Drug Discov. 3 (2004) 1023–1035, https://doi.org/10.1038/nrd1576.

[29] B. Tian, Y. Liu, J. Liu, Smart stimuli-responsive drug delivery systems based on cyclodextrin: A review, Carbohyd. Polym. 251 (2021), https://doi.org/10.1016/j.carbpol.2020.116871.

[30] J. Wankar, N.G. Kotla, S. Gera, S. Rasala, A. Pandit, Y.A. Rochev, Recent advances in host–guest self-assembled cyclodextrin carriers: implications for responsive drug delivery and biomedical engineering, Adv. Funct. Mater. 30 (2020), https://doi.org/10.1002/adfm.201909049.

[31] S. Panda, S. Fourmentin, Cyclodextrin-based supramolecular low melting mixtures: efficient absorbents for volatile organic compounds abatement, Environ. Sci. Pollut. R. 29 (2022) 264–270, https://doi.org/10.1007/s11356-021-16279-y.

[32] A. Triolo, F. Lo Celso, S. Fourmentin, O. Russina, Liquid structure scenario of the archetypal supramolecular deep eutectic solvent: heptakis(2,6-di-O-methyl)-β-cyclodextrin/levulinic acid, ACS Sustain, Chem. Eng. 11 (2023) 9103–9110, https://doi.org/10.1021/acssuschemeng.3c01858.

[33] M. Kfoury, D. Landy, S. Fourmentin, Combination of DES and macrocyclic host molecules: Review and perspectives, Curr. Opin. Green Sustain. 36 (2022), https://doi.org/10.1016/j.cogsc.2022.100630.

[34] P. Blach, S. Fourmentin, D. Landy, F. Cazier, G. Surpateanu, Cyclodextrins: A new efficient absorbent to treat waste gas streams, Chemosphere 70 (2008) 374–380, https://doi.org/10.1016/j.chemosphere.2007.07.018.

[35] T. Moufawad, L. Moura, M. Ferreira, H. Bricout, S. Tilloy, E. Monflier, M. Costa Gomes, D. Landy, S. Fourmentin, First evidence of cyclodextrin inclusion complexes in a deep eutectic solvent, ACS Sustain, Chem. Eng. 7 (2019) 6345–6351, https://doi.org/10.1021/acssuschemeng.9b00044.

[36] M.E. Di Pietro, G. Colombo Dugoni, M. Ferro, A. Mannu, F. Castiglione, M. Costa Gomes, S. Fourmentin, A. Mele, Do cyclodextrins encapsulate volatiles in deep eutectic systems?, ACS Sustain, Chem. Eng. 7 (2019) 17397–17405, https://doi.org/10.1021/acssuschemeng.9b04526.

[37] L. Moura, T. Moufawad, M. Ferreira, H. Bricout, S. Tilloy, E. Monflier, M.F. Costa Gomes, D. Landy, S. Fourmentin, Deep eutectic solvents as green absorbents of volatile organic pollutants, Environ. Chem. Lett. 15 (2017) 747–753, https://doi.org/10.1007/s10311-017-0654-y.

[38] A.S. Rodriguez Castillo, P.F. Biard, S. Guihéneuf, L. Paquin, A. Amrane, A. Couvert, Assessment of VOC absorption in hydrophobic ionic liquids: Measurement of partition and diffusion coefficients and simulation of a packed column, Chem. Eng. J. 360 (2019) 1416–1426, https://doi.org/10.1016/j.cej.2018.10.146.

[39] B. Kolb, L.S. Ettre, Static headspace-gas chromatography: Theory and practice, Wiley (2006), https://doi.org/10.1002/0471914584.ch2.

[40] D. Landy, S. Fourmentin, M. Salome, G. Surpateanu, Analytical improvement in measuring formation constants of inclusion complexes between β-cyclodextrin and phenolic compounds, J. Incl. Phenom. Macro. 38 (2000) 187–198, https://doi.org/10.1023/A:1008156110999.

[41] M.J. Frisch, G.W. Trucks, H.B. Schlegel, Gaussian 09, Revision D. 01, Gaussian, (2009). http://www. gaussian. com/.

[42] J. Da Chai, M. Head-Gordon, Long-range corrected hybrid density functionals with damped atom-atom dispersion corrections, PCCP 10 (2008) 6615–6620, https://doi.org/10.1039/b810189b.

[43] S. Soleimani-Amiri, M. Koohi, Z. Azizi, Characterization of nonsegregated C17Si3 heterofullerenic isomers using density functional theory method, J. Chin. Chem. Soc. 65 (2018) 1453–1464, https://doi.org/10.1002/jccs.201800163.

[44] T. Lu, F. Chen, Multiwfn: A multifunctional wavefunction analyzer, J. Comput. Chem. 33 (2012) 580–592, https://doi.org/10.1002/jcc.22885.

[45] D. Van Der Spoel, E. Lindahl, B. Hess, G. Groenhof, A.E. Mark, H.J.C. Berendsen, GROMACS: Fast, flexible, and free, J. Comput. Chem. 26 (2005) 1701–1718, https://doi.org/10.1002/jcc.20291.

[46] J. Huang, A.D. Mackerell, CHARMM36 all-atom additive protein force field: Validation based on comparison to NMR data, J. Comput. Chem. 34 (2013) 2135–2145, https://doi.org/10.1002/jcc.23354.

[47] J. Wang, R.M. Wolf, J.W. Caldwell, P.A. Kollman, D.A. Case, Development and testing of a general Amber force field, J. Comput. Chem. 25 (2004) 1157–1174, https://doi.org/10.1002/jcc.20035.

[48] W.L. Jorgensen, J. Chandrasekhar, J.D. Madura, R.W. Impey, M.L. Klein, Comparison of simple potential functions for simulating liquid water, J. Chem. Phys. 79 (1983) 926–935, https://doi.org/10.1063/1.445869.

[49] P. Villarim, C. Gui, E. Genty, Z. Lei, J. Zemmouri, S. Fourmentin, Toluene absorption from laboratory to industrial scale: An experimental and theoretical study, Sep. Purif. Technol. 328 (2024), https://doi.org/10.1016/j.seppur.2023.125070.

[50] D.T. Leighton, J.M. Calo, Distribution coefficients of chlorinated hydrocarbons in dilute air-water systems for groundwater contamination applications, J. Chem. Eng. Data 1981 (1881) 382–385, https://doi.org/10.1021/JE00026A010.

[51] J.M. Gossett, Measurement of Henry's law constants for C1 and C2 chlorinated hydrocarbons, Environ. Sci. Tech. 21 (1987) 202–208, https://doi.org/10.1021/es00156a012.

[52] A.P. Karman, S.E. Ebeler, N. Nitin, S.R. Dungan, Partitioning, solubility and solubilization of limonene into water or short-chain phosphatidylcholine solutions, J. Am. Oil Chem. Soc. 98 (2021) 979–992, https://doi.org/10.1002/aocs.12535.

[53] J.L. Hamelink, P.B. Simon, E.M. Silberhorn, Henry's Law Constant, Volatilization Rate, and Aquatic Half-Life of Octamethylcyclotetrasiloxane, Environ. Sci. Tech. 30 (1996) 1946–1952, https://doi.org/10.1021/es950634j.

[54] S. Fourmentin, M. Outirite, P. Blach, D. Landy, A. Ponchel, E. Monflier, G. Surpateanu, Solubilisation of chlorinated solvents by cyclodextrin derivatives. A study by static headspace gas chromatography and molecular modelling, J. Hazard. Mater. 141 (2007) 92–97, https://doi.org/10.1016/j.jhazmat.2006.06.090.

[55] A. Triolo, F. Lo Celso, O. Russina, Structural features of β-cyclodextrin solvation in the deep eutectic solvent, reline, J. Phys. Chem. B 124 (2020) 2652–2660, https://doi.org/10.1021/acs.jpcb.0c00876.

[56] V.Y. Rudyak, A.A. Belkin, D.A. Ivanov, V.V. Egorov, The simulation of transport processes using the method of molecular dynamics, Self-Diffusion Coefficient, High Temp+. 46 (2008) 35–44, https://doi.org/10.1134/S0018151X08010069.

[57] F. Bayat, S.S. Homami, A. Monzavi, M.R. Talei Bavil Olyai, A combined molecular docking and molecular dynamics simulation approach to probing the host–guest interactions of Ataluren with natural and modified cyclodextrins, Mol. Simulat. 48 (2022) 108–119, https://doi.org/10.1080/08927022.2021.1991921.

[58] J. Perez-Miron, C. Jaime, P.M. Ivanov, Molecular dynamics study on the conformational flexibility and energetics in aqueous solution of methylated β-cyclodextrins, Chirality 20 (2008) 1127–1133, https://doi.org/10.1002/chir.20571.

[59] B. Li, C. Wang, Y. Zhang, Y. Wang, High CO_2 absorption capacity of metal-based ionic liquids: A molecular dynamics study, Green, Energy Environ. 6 (2021) 253–260, https://doi.org/10.1016/j.gee.2020.04.009.

[60] S.B. Pour, J.J. Sardroodi, A.R. Ebrahimzadeh, Structure and dynamics of thymol - fatty acids based deep eutectic solvent investigated by molecular dynamics simulation, Fluid Phase Equilib. 552 (2022), https://doi.org/10.1016/j.fluid.2021.113241.